Pavement temperature mitigation by the means of geothermally and solar heated air

A. Chiarelli*, A.R. Dawson, A. García

Nottingham Transportation Engineering Centre (NTEC), Faculty of Engineering, The University of Nottingham, University Park, Nottingham, NG7 2RD

Abstract

In this article, a novel method to mitigate pavement temperatures by the means of air convection is presented. The technique introduced here is based on a new type of experimental setup called a ground source heat simulator, which is able to feed air at a controlled temperature to a set of pipes embedded under a test pavement surface. The air at the chosen temperature can flow through the designed system by natural convection. The air heated by the simulated geothermal source can mitigate the pavement temperature in winter and summer conditions in order to avoid freezing and overheating of paving surfaces in an urban environment. In particular, during winter the geothermal air warms up the pavement, while during summer the pavement is cooled down. Laboratory tests of the ground source heat simulator allowed the collection of a high amount of data, which is here analysed statistically and computationally. This article shows that the use of geothermal energy to preheat the inlet air in pavements where an array of pipes is installed can provide a measurable contribution for the mitigation of pavement temperatures in both winter and summer conditions. Furthermore, the experimental data gathered successfully proved the effectiveness of computational simulations for the study of buoyancy powered air flow through channels buried under pavements and increased the understanding

*Corresponding author

Email addresses: chiarelli.andrea@gmail.com (A. Chiarelli), andrew.dawson@nottingham.ac.uk (A.R. Dawson), alvaro.garcia@nottingham.ac.uk (A. García)

of the physical phenomena happening in the system under analysis. Finally, preliminary testing in the environment showed that the concept is effective and works as expected.

Keywords: air convection, temperature mitigation, geothermal, asphalt pavement, environment

1. Introduction

In the past few years, the relationship between pavement temperatures and the built environment has been studied by a number of researchers. Pavement temperatures are mostly determined by the ambient temperature, which is variable across the year for all the areas in the so-called temperate zone [1]. During cold periods, when the temperature is low for a long period of time and snow is present on the pavement surface, it is common to observe the formation of ice. The presence of ice on roads creates hazards for people and vehicles [2, 3], and thus it often leads to traffic blocks and subsequent loss of functional availability of the road infrastructure. The presence of ice or snow is also an issue for airports, where it can have a serious impact on the safety of take-off and landing operations [3, 4]. Furthermore, in some situations, the presence of snow alone may be enough to make local authorities forbid vehicle circulation due to the fear of traffic accidents.

On the other hand, during hot periods, high pavement temperatures are known to allow the development of rutting and structural damage [5]. In addition, high pavement temperatures increase the urban heat island (UHI) effect, thus, causing further issues related to a high consumption of energy by air conditioning systems in cities during summer [6]. Therefore, high pavement temperatures during summer can lead to hazards in the transport infrastructure, reducing its reliability, and also contribute to additional stress on the energy distribution network.

Since in the current economy the availability of the road network for the delivery of goods is essential, methods for de-icing or snow melting during winter and for the reduction of surface temperatures during summer are of increasing importance. In the case of winter, two main solutions exist for these purposes, i.e., the use of chemical substances [2, 3] and the use of pipes where a hot fluid (typically water with an antifreeze additive) is circulated after being heated geothermally [7, 8]. The first method has been used for a long time now and it is regarded as a very effective method, however it has recently been raising concerns about its effect on the environment [3, 9]. On the other hand, the use of piping systems still has to be explored extensively and few examples exist in Argentina, Iceland, Japan, Switzerland, and U.S.A. [8]. In addition, piping systems buried below the wearing course of a pavement are known to cause serious durability problems in the case of a water leakage [10, 11], which also requires the remediation of non-aqueous phase liquids (NAPLs) in the subsurface when an antifreeze additive is used [12]. In the case of summer conditions, more methods to mitigate the pavement temperatures have been studied, e.g., the use of energy harvesting pavements [10, 11, 13, 14, 15] or changes in the materials properties such as thermal conductivity, specific heat capacity, albedo, or emissivity [6, 16, 17, 18, 19, 20, 21, 22, 23, 24].

Since the use of piping systems buried under the pavement surface has been considered for both cold and warm periods, in this paper, the use of an energy harvesting pavement powered by air convection is considered for the mitigation of extreme temperature effects during the whole year. This could potentially deliver similar benefits as a water based system, but without the durability and leakage concerns. Nonetheless, it must be noted that the use of air may cause some concerns, as this fluid performs worse than water in terms of heat transfer due to its poorer thermodynamic properties. In addition, since the air flow through buried pipes is influenced by a variable heat gradient (due to varying external temperatures), its control may prove difficult. Thus, the practical design of the system could become complex.

The experimental layout used in the present work is based on a convection powered energy harvesting pavement, which consists of a set of pipes buried under the asphalt wearing course [13, 10, 11]. The use of a simulated geothermal heat source is considered in this paper to control the inlet temperature for the above-mentioned energy harvesting prototype. For this purpose, a novel experimental setup called a ground source heat simulator was built at the Nottingham Transportation Engineering Centre (NTEC) and used to reach a number of temperatures meant to simulate the soil temperatures at a range of depths. The ground source heat simulator is here meant to generate a representative mass of air at thermal equilibrium with the soil.

1.1. Research objectives

The main aims of the present study are (i) to assess if it is possible to control (increase or decrease) effectively the surface temperature of a pavement through the use of air warmed up by geothermal resources, and (ii) to quantify the increase or decrease in the pavement temperature through the use of natural convection powered by geothermal or solar heat sources.

These objectives were pursued by running a number of experiments based on the use of a ground source heat simulator (see Fig. 1). The experimental results were also used to develop a modelling approach for the study of the design of buoyancy powered flow in pavements where an array of pipes or channels is installed. Furthermore, preliminary testing in the environment was carried out at the University of Nottingham, UK campus in order to verify the validity of the approach in a more realistic scenario.

2. Methodology

2.1. Concept of a ground source heat simulator

In this paper, a ground source heat simulator is described for the analysis of the temperature control potential in pavements where an array of pipes is installed. A possible real apparatus for the exploitation of geothermal heat for the purposes mentioned in the Introduction is shown in Fig. 2(a). The figure shows that an air inlet could be allowed, e.g., in the soft shoulder of a pavement. Such an inlet would consist of a pipe installed beneath the pavement at a certain

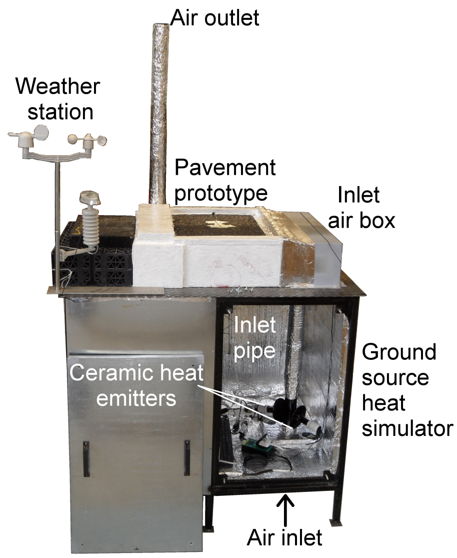

Figure 1: Ground source heat simulator built at the Nottingham Transportation Engineering Centre (NTEC).

depth, which would act as a heat exchanger transferring heat from the ground (geothermal heat) to the air. The pipe would then rise closer to the pavement wearing course, where it would exchange heat with the asphalt surface. Finally, the air would flow through a chimney and return to the environment. The significance of this concept lies in the fact that geothermal heat alone cannot influence strongly the pavement surface due to its low temperature and depth. However, the above-mentioned layout exploits air to carry geothermal heat to the surface and potentially mitigate or solve the engineering issues related to the maintenance of paved surfaces and mentioned in the Introduction.

The ground source heat simulator is meant to show how geothermal heat can affect the pavement temperature during the whole year, when the external environment may be either cold or warm. During cold periods, geothermal heat would power the air flow by heating up the air in the pipes and, thus, decreasing its density. Geothermal heat would drive a convective air flow from the inlet to

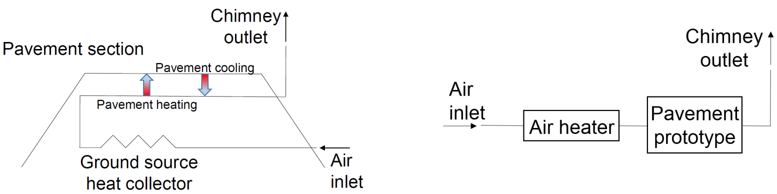

(a) Hypothetical full scale apparatus for the management of pavement temperatures.

(b) Laboratory setup of a ground source heat simulator.

Figure 2: Hypothesised system and installation scheme vs. Laboratory setup.

the pavement surface, where the air would lose some thermal energy and release it to the paving materials. On the other hand, during warm periods, the air flow (and ensuing heat transfer) would be driven by the high surface temperature of the pavement and the ground surrounding the buried inlet pipe would act as a heat accumulator [7]. This would be helpful for the winter performance, as the accumulated heat would delay the moment when ice first starts forming on the pavement surface.

Note that this section only offers a hypothetical description of a possible real life layout of the technology. At this stage, it is not possible to deepen the discussion of engineering and practical construction matters, as the system is yet to be fully tested and analysed.

2.2. Structure of the ground source heat simulator

In order to assess the feasibility of the concept described in Section 2.1, a ground source heat simulator was built following the scheme shown in Fig. 2(b).

The size of the pavement prototype represented in Fig. 1 is 470 mm x 700 mm x 180 mm [25]. As shown in Fig. 3, the pavement prototype consists of two layers. The asphalt wearing course (exposed to the environment) was built with a dense mixture (limestone, maximum size 11 mm), while the bottom layer consists of coarse limestone gravel and includes the stainless steel pipes used to allow the air flow.

The ground source heat simulator (see Fig. 1) was installed in a stainless steel cabinet 1300 mm long, 1000 mm wide, and 1200 mm high. On the roof, a stainless steel box open on two sides was installed to allow the movement of air from the ground source heat simulator to the above-mentioned pavement prototype. Because of its role, the steel box on the roof will be regarded as the inlet air box from this point onwards. More details on the path of air in the ground source heat simulator can be found in Section 2.3.

All the sides of the ground source heat simulator and the inlet air box were thoroughly insulated in order to allow a precise temperature control with negligible influence from the surrounding environment. The insulation material is 25 mm thick extruded polystyrene foam covered with sheets of aluminium bubble foil insulation.

As shown in Fig. 3 and Fig. 4, thermocouples (K-type) were used to measure the temperatures on the asphalt surface, 50 mm from the top of the surface, 50 mm from the bottom of the aggregate layer of the prototype pavement, and in the inlet air box. In addition, the environmental conditions were monitored with a weather station (PCE-FWS 20).

Finally, it is relevant to add that the use of a temperature controlled extractor fan is necessary to keep the internal volume of the cabinet below temperatures that might affect the data logging equipment (OMEGA OMB-DAQ-54) or cause unsafe operating conditions.

2.3. Generation of the air flow

A stainless steel vertical pipe (inlet pipe in Fig. 1) was installed to connect the bottom surface of the ground source heat simulator to the centre of the inlet air box. The role of the inlet pipe is to provide an air mass flow to the pavement prototype that is to be tested. The inlet pipe is connected to the environment on the bottom side of the steel box and no exchange of air is allowed between its inner volume and the internal part of the ground source heat simulator cabinet. This layout was chosen in order to allow the direct control of the temperature inside the inlet air box by the use of 250W ceramic heat emitters connected to a

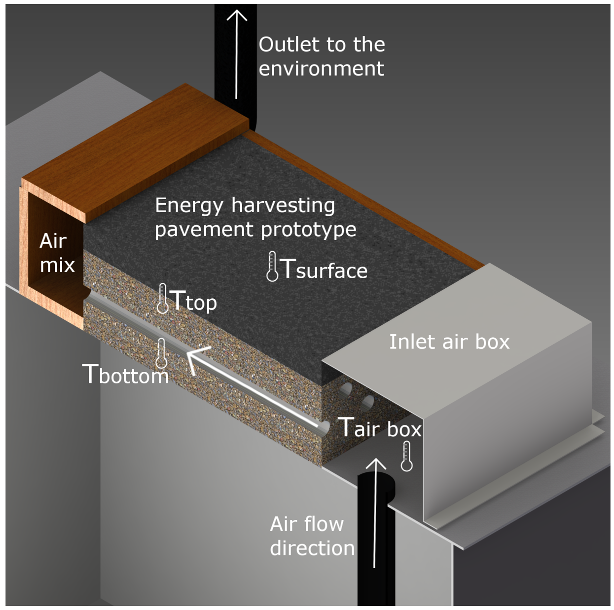

Figure 3: Path of the air flow and position of the thermocouples (cross section).

thermostat and facing the inlet pipe (see Fig. 1). The use of heating elements is a key aspect in the experimental setup, as this is what allows the simulation of a heat exchange with a geothermal resource and provides the driving force for natural convection of air. The thermostat for the regulation of the temperature in the inlet air box is equipped with a probe placed at the outlet of the inlet pipe. This configuration allows the user to set a temperature threshold for the inlet air box, thus, preventing the temperature from dropping below a desired value.

2.4. Energy harvesting prototype

The inlet air box is the part connecting the ground source heat simulator to the pavement prototype described in Chiarelli et al. [11, 10]. With reference to Fig. 3, environmental air heated by the ceramic heat emitters flows upwards through the inlet pipe to the inlet air box, goes through the pavement prototype via an array of pipes, mixes in the air mixing box situated at the outlet of the pipes, and finally exits the system through a chimney.

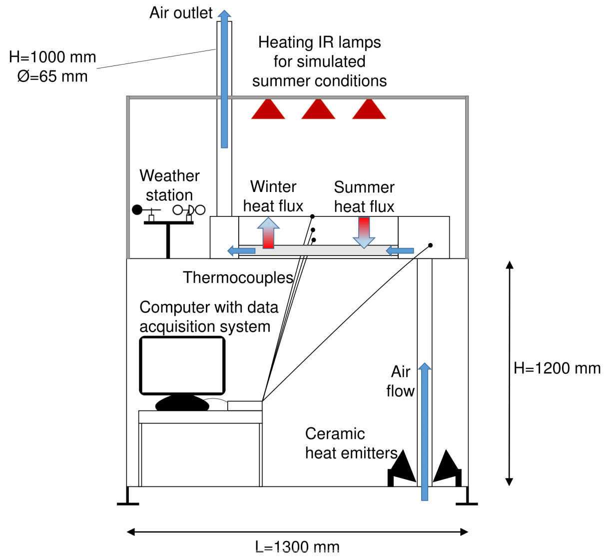

Figure 4: Simplified scheme of the ground source heat simulator.

Air from the ground source heat simulator is meant to release or absorb heat from the pavement, depending on the external conditions. If infrared lamps are used to heat up the pavement surface [11, 10] (see Fig. 3), summer conditions are simulated, while if the pavement is at ambient or cooled temperature, winter conditions are considered.

The chimney height and internal diameter are respectively 1000 mm and 65 mm, as this was recognised as an overall efficient configuration considering temperature reduction efficiency and energy efficiency in a previous study [11].

2.5. Experiments performed

Due to the fact that the experiments were performed in a laboratory, approximations were necessary to reproduce winter and summer conditions. In particular, it was decided to simulate each season based on the temperature difference between the pavement surface and the simulated heat source. In the simulation of summer conditions, a maximum surface temperature of about 78°C was reached during test trials by the use of infrared heating elements [11]. This value is about 10°C higher than maximum summer pavement temperatures determined by Pascual-Muñoz et al. [14]. Thus, it was decided to use simulated reservoir temperatures 10°C higher than realistic ones. Due to this, a range between 22 °C and 36 °C was chosen as the inlet temperature to reproduce equivalent inlet temperatures of 12°C and 26°C. The lower end of the interval is meant to simulate a normal soil temperature, while the higher end represents the use of exhaust heat from a hypothetical building. For clarity all the experimental conditions considered are gathered in Table 1.

In the case of winter conditions, the experimental setup was limited by the fact that the equipment could not reach real winter temperatures. Therefore, ambient temperature (about 20.5°C) was considered as the winter temperature, while the reservoir temperatures were fixed between 23°C and 30°C. This means that the equivalent winter inlet temperatures considered range between about 2.5°C and 9.5°C.

It is relevant to notice that the minimum equivalent reservoir temperature for summer (12°C) is slightly higher than that for winter (9.5°C): this was done to account for the seasonal variation in the reservoir temperature at a given depth, which is higher in summer than in winter. Lower summer reservoir temperatures were not considered because of limitations in the experimental equipment, which cannot generate an inlet temperature below ambient temperature.

Finally, for the analysis of winter conditions the surface temperature of a control asphalt slab where no channels for air flow were installed was measured along with the other temperatures being considered. This was done in order to provide data about the effectiveness of the system, as a simple comparison allows the quantification of the temperature control potential of the experimental setup considered. This comparison was not performed for summer conditions, as data on this is already available in the literature [11, 10] and the actual performance depends on a number of design choices that are not taken into account in this paper. In simulated summer conditions, however, a test with blocked pipes was run (therefore, with no air convection under the pavement), obtaining a maximum temperature of about 80°C that can be used for comparison purposes.

All laboratory experiments were performed in dry conditions. This choice was

Simulated conditions	Inlet temperatures tested (°C)								IR lamps on surface
Winter	23	24	25	26	27	28	29	30	Off
Summer	22	24	26	28	30	32	34	36	On

Table 1: Experiments performed

made because in moist conditions evaporation phenomena would influence the energy available for harvesting or used in heating the pavement [26], thus, it would be very complicated to find out if a given surface temperature is caused by water evaporation, by energy harvesting, by pavement heating, or by some combination of these functions.

3. Statistical and computational methods

3.1. Description of the relevant physical phenomena

In the study of convection powered air flows in channels installed under the surface of pavements, the main physical phenomena at work are heat and mass transfer [11]. In particular, heat is transmitted from the sun to the pavement, and from the pavement to the operating fluid. The fluid moves in the channels installed in layers in or under the pavement thanks to differences in the air density between the inlet and the outlet of the system, i.e., the fluid flow is originated by air buoyancy.

In a previous study, it was shown that an approach based only on heat flow does not provide a satisfactory description of the physics of energy harvesting pavements [11]. For this reason, it is necessary to additionally describe fluid flow in the system. In particular, the analysis of energy harvesting powered by air convection needs to be performed by combining the First Law of Thermodynamics and the Navier-Stokes equations with the equation of mass conservation, therefore, considering energy, momentum, and continuity in the system, respectively.

First, since the flow is considered as incompressible, the formulation of the First Law of Thermodynamics, or energy equation, in three dimensions [27] is written as:

$$\rho c_p \frac{\partial T}{\partial t} + \rho c_p u \frac{\partial T}{\partial x} + \rho c_p v \frac{\partial T}{\partial y} + \rho c_p w \frac{\partial T}{\partial z} = \frac{\partial}{\partial x}\left[k \frac{\partial T}{\partial x}\right] + \frac{\partial}{\partial y}\left[k \frac{\partial T}{\partial y}\right] + \frac{\partial}{\partial z}\left[k \frac{\partial T}{\partial z}\right] + q_v \tag{1}$$

The variables used in Eq. 1 are defined in Table 2.

Second, the momentum equation for the x direction [27] is:

$$\rho \frac{\partial u}{\partial t} + \rho u \frac{\partial u}{\partial x} + \rho v \frac{\partial u}{\partial y} + \rho w \frac{\partial u}{\partial z} = \rho g_x - \rho \frac{\partial p}{\partial x} + \frac{\partial}{\partial x}\left[2\mu \frac{\partial u}{\partial x}\right] + \frac{\partial}{\partial y}\left[\mu \left(\frac{\partial u}{\partial y} + \frac{\partial v}{\partial x}\right)\right] + \frac{\partial}{\partial z}\left[\mu \left(\frac{\partial u}{\partial z} + \frac{\partial w}{\partial x}\right)\right] \tag{2}$$

The formulation for the other directions can be easily adapted from Eq. 2 and the variables used are gathered in Table 2. It is relevant to point out that since the convective air flow is originated by buoyancy the gravity term in Eq. 2, ρg_x, is expected to dominate the flow.

Third, the physical description of the system is completed by using a continuity equation, also referred to as the equation of mass conservation [27]:

$$\frac{\partial \rho}{\partial t} + \frac{\partial \rho u}{\partial x} + \frac{\partial \rho v}{\partial y} + \frac{\partial \rho w}{\partial z} = 0 \tag{3}$$

In this paper, steady state conditions are considered due to the need to reproduce steady state experimental results. Therefore, Eqs. 1, 2, and 3 can be simplified by neglecting the time-dependent terms, i.e., all the terms showing ∂t in the denominator. Moreover, the volumetric heat generation term, q_v, in Eq. 1 can be neglected, as there are no heat sources or sinks within the pavement.

Furthermore, it is very important to keep in mind that the air flow in the prototype pavement considered in this paper is a density driven phenomenon, therefore, it is mandatory to allow the density of air to change based on its physical state. The variation of the density can be computed through Boussinesq's approximation [28, 29, 30] or the low Mach number assumption [28, 31]. In this paper, the low Mach number assumption is considered, thus, the pressure to use in Eq. 1 for all the directions is written as:

$$p = P_{ref} + \rho_\infty g_i x_i + p^* \tag{4}$$

Variable	Physical meaning	Unit
ρ	density of fluid (air) in the system	kg/m^3
c_p	specific heat capacity	$J/(kgK)$
T	temperature	K
t	time	s
u	velocity in x-direction	m/s
v	velocity in y-direction	m/s
w	velocity in z-direction	m/s
k	thermal conductivity	$W/(mK)$
q_v	heat source	W/m^3
g_x	gravitational acceleration in x direction	m/s^2
μ	dynamic viscosity	$kg/(ms)$

Table 2: Variables used in Eq. 1 and Eq. 2.

where P_{ref} is the atmospheric pressure, ρ_∞ is the density at ambient temperature and pressure, g_i is the gravity vector, and x_i is the distance vector from the origin. Due to the use of Eq. 4, p^* becomes the variable describing the pressure in the momentum equations.

All the equations described in this Section can be combined to computationally describe the physics in a temperature modifying pavement. Further details on this aspect can be found in Section 3.3.

3.2. Statistical analysis of the experimental results

In previous work by the authors, it was shown that simplified theoretical models are not fit to represent the wide variety of thermophysical phenomena that happen in the energy harvesting pavement under investigation [11].

It is, however, possible to analyse the relationship between all the parameters of interest in the system in order to (i) find out which variables have the highest influence on the behaviour of the prototype and (ii) to check whether the application of the abovementioned equations is fit to represent the phenomena at work. A simple and effective way to study the relationship (if any) between the measured data is the use of the dimensionless index called the Pearson's correlation coefficient [32, 33, 34] (or Pearson's r), which provides a measure of the linear dependence between two variables. This coefficient ranges between -1 and +1, where -1 means that there is a total negative correlation and +1 means that there is a total positive correlation between the variables [35, 32].

Generally speaking, a value of the Pearson's coefficient close to -1 or +1 is a sign that a negative or positive linear relationship exists between the data being considered. In this paper, values below -0.8 or above +0.8 are considered as an indication of a strong linear relationship between the data, while values outside this interval are considered as the sign of a moderate or weak correlation [33, 34]. No actual distinction is here made between the values in the interval $-0.8 < r < 0.8$, as they are not relevant for the purposes of this study.

The level of significance (2-tailed) of the results is reported along with the values of the Pearson's correlation coefficient for all the parameters investigated [34, 36]. The choice of a 2-tailed test is motivated by the fact that no consistent directionality was seen in the raw data [36] and because the relationship between the datasets needs to be investigated in both directions in order to be able to provide accurate conclusions.

3.3. Computational reproduction of temperature modifying pavements

Along with a study of the relative influence of the parameters of interest in the system, a computational analysis of the temperature modifying setup was performed. In this paper, coupled heat and mass transfer are used to (i) reproduce the experimental results obtained with the experimental setup under analysis and (ii) to study possible improvements to the design of the prototype being investigated. These purposes were pursued by the means of computational fluid dynamic (CFD) simulations run with the software Autodesk CFD. The experimental setup was built as a 3D domain and meshed (see Fig. 5), then the relevant boundary conditions were applied to run the simulations. The reproduction of the experimental results was meant to assess the effectiveness of Eq. 1, Eq. 2, and Eq. 3 for the description of convection powered air flows

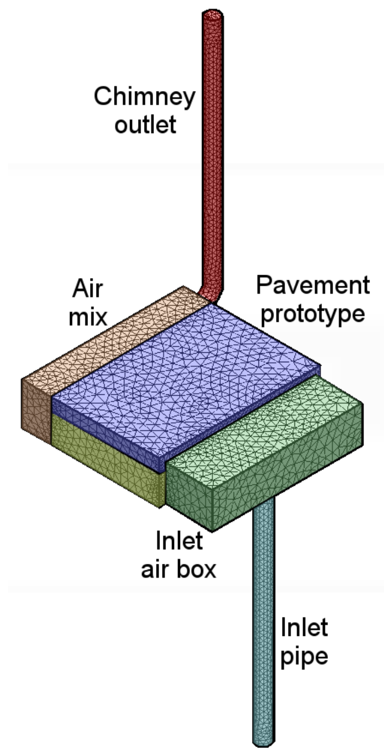

Figure 5: Meshed 3D model of the prototype pavement studied.

in channels installed under pavements and to tune the computational setup of the problem. When this was achieved, fluid dynamics in the domain could be effectively studied and the possible weaknesses of the experimental setup identified.

3.3.1. Boundary conditions in the computational study

The computational domain considered for the study of thermo-fluid dynamics in the pavement prototype consists of the inlet pipe, the inlet air box, the pavement prototype, and the chimney outlet. This choice was motivated by the fact that the shape of the air channels is expected to influence the air flow in the system, since it includes a number of sharp turns. The presence of sharp turns (see, e.g., Fig. 3) is a clear indication that, based on the air speed, there will be head losses in the system.

In order that the results of the CFD model are not constrained by assumed boundaries that significantly differ from those actually experienced by the prototype pavement the boundary conditions used were the measured surface temperature in steady state, the temperature set at the inlet, and the environmental temperature at the end of the physical tests. Furthermore, the presence of the environmental pressure at the system inlet and outlet was considered by setting a gauge pressure equal to zero in both these openings.

It is important to keep in mind that the laboratory conditions allow phenomena such as surface convection and not perfectly constant ambient temperatures (even if in a small range), which were neglected in the computational problem setup. Therefore, the computational results are not expected to be an exact match to the experimental ones.

Since all the relevant temperatures are here used as boundary conditions, the computational results are compared to the experimental ones based on the outlet air speed. If the air speed was fixed, any other temperature of interest could be estimated based on the equations listed in Section 3.1.

4. Results and discussion

4.1. Experimental results

The experiments run for this paper produced a very high amount of data, thus, only selected results are graphically shown in order to allow an understanding of the phenomena at work and to facilitate comparison with the existing literature [11, 10]. It is very important to focus on the fact that the temperature modifying setup considered here has two different roles in simulated winter and summer conditions, i.e., in winter the air flow releases heat to the pavement, while in summer the system removes thermal energy. For this reason, in order to understand the experimental results two different approaches must be followed. In the case of simulated winter conditions, the focus is on the increase in the surface temperature of the pavement prototype compared to

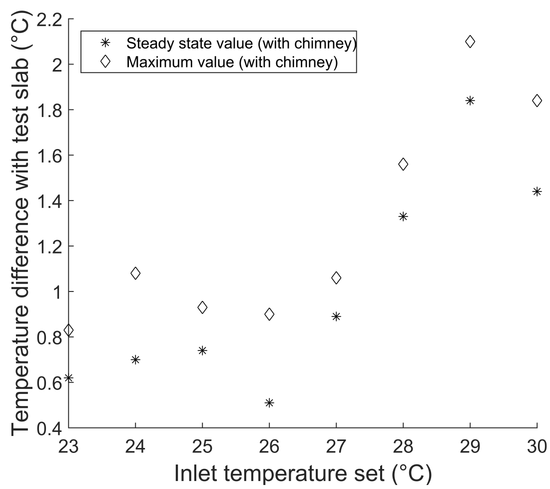

(a) Tests with chimney

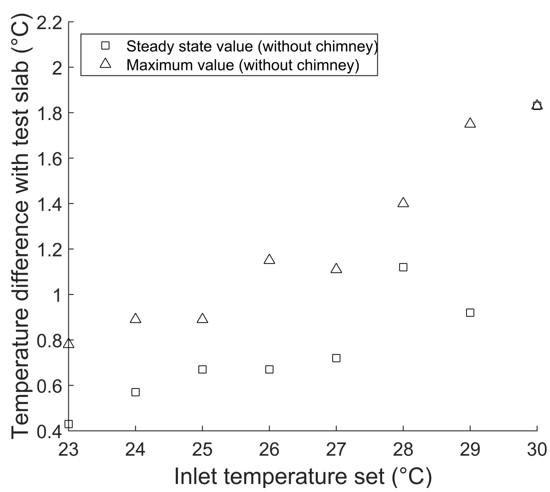

(b) Tests without chimney

Figure 6: Temperature differences with control slab (Laboratory simulated winter conditions).

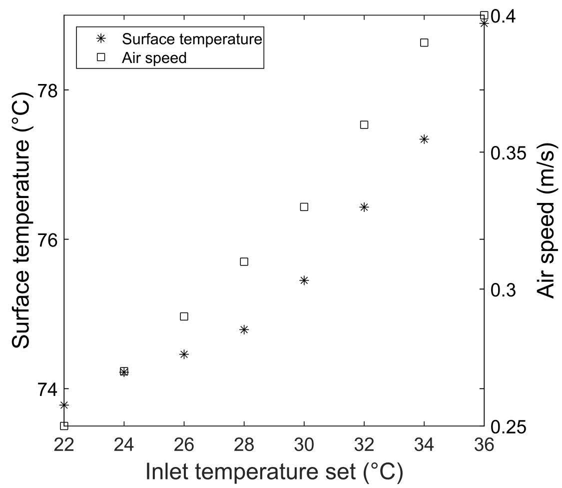

Figure 7: Surface temperature and air speed vs. Set inlet temperature (Laboratory simulated summer conditions, with chimney).

a traditional pavement, which can provide an estimation of the effectiveness of the experimental setup. On the other hand, during simulated summer conditions, the most interesting parameters are the outlet air speed and the surface temperature, which are related to the amount of energy that is extracted from the pavement [11, 10].

The experimental data concerning the temperature differences in simulated winter conditions is shown in Fig. 6, while the surface temperatures and air speeds for summer are represented in Fig. 7. A quick look at Fig. 6 and Fig. 7 suggests that higher inlet temperatures always result in higher values on the relevant parameters shown on the y axes in both winter and summer simulated conditions. A small scatter of the points can be observed in simulated winter conditions, however, this is an effect of the slightly varying environmental conditions, which cannot be kept in a perfectly stable thermodynamic state. As a result, the trend in the data may seem not to be as clear as in the simulated summer conditions. By comparing Fig. 6(a) with Fig. 6(b) it can also be observed that the results in winter conditions are not highly influenced by the presence of the chimney. Moreover, as a proof of the effectiveness of the concept shown in Fig. 2, it can be observed that temperature differences obtained in winter conditions range between 0.4°C and 2.1°C. On the other hand, since the maximum pavement temperature with no energy abstraction in simulated summer conditions was 80°C, temperature reductions between 2°C and 6°C were achieved.

It is interesting to notice that data in previous experiments showed that the air speed in summer conditions reached a peak value corresponding to a chosen configuration (chimney height, chimney diameter) of an energy harvesting pavement prototype [11], while this is not seen in Fig. 7. The reason for the different behaviour is that in the current experimental investigation the layout of the system was kept constant, thus, the air speed was solely influenced by the inlet temperature, which did not cause any local maximum or minimum point for the air speed in the range considered.

The other data gathered in the experiments and not graphically represented in the current Section is analysed more in detail in the next Section 4.2, where the correlation between all the parameters considered is investigated.

It is important to highlight that the use of equivalent temperatures proposed in this paper is not an exact approach, as weather conditions are not defined only by temperature differences, however, the approximation was deemed acceptable for the first tests run with this novel experimental setup. If a temperature difference is considered between the air entering the pipes and the surface temperature, the energy absorbed by the operating fluid is expected to approximate in-situ conditions. This is because this amount of energy depends on the heat transfer phenomena happening in the pavement prototype and on temperature differences rather than on temperatures alone.

4.2. Statistical analysis

The experimental data gathered was used to calculate the Pearson's correlation coefficient between all the parameters under analysis. The results of the statistical analysis are reported in the next Sections separately for winter and summer conditions.

	T_s	ΔT_{max}	ΔT_f	v_a	$T_{control}$	T_b	T_{top}	$T_{air\ box}$	T_{set}
T_s	1								
ΔT_{max}	0.129	1							
ΔT_f	-0.275	0.846**	1						
v_a	-0.079	0.850**	0.835**	1					
$T_{control}$	0.959**	-0.137	-0.536	-0.316	1				
T_b	0.739*	0.734*	0.365	0.573	0.541	1			
T_{top}	0.996**	0.154	-0.273	-0.051	0.955**	0.752*	1		
$T_{air\ box}$	0.518	0.837**	0.557	0.766*	0.290	0.949**	0.531	1	
T_{set}	0.123	0.961**	0.853**	0.933**	-0.144	0.753*	0.141	0.891**	1

*Correlation is significant at the 0.05 level (2-tailed).
**Correlation is significant at the 0.01 level (2-tailed).

Legend:
T_s=surface temperature of prototype pavement, $T_{control}$= surface temperature of control slab,
$\Delta T_{max} = max(T_s - T_{control})$, $\Delta T_f = (T_s - T_{control})_{steady\ state}$,
v_a= air speed, T_b= temperature at 50 mm from bottom of prototype pavement,
T_{top}= temperature at 50 mm from surface of prototype pavement,
$T_{air\ box}$= temperature at inlet air box, T_{set}= inlet temperature chosen

Table 3: Pearson's correlation coefficient for the simulation of winter conditions.

4.2.1. Winter conditions

The Pearson's r is reported in Table 3 along with the statistical significance for all the parameters studied in winter conditions. The results are analysed for the whole data gathered, considering experiments with and without chimney because a preliminary assessment of the data suggested that in winter conditions (i.e., with small or negligible incident radiation) the presence of the chimney does not highly influence the results.

As can be observed in Table 3, the analysis of the Pearson's correlation coefficient suggests that many linear correlations exist between the data under investigation. The most important result is the fact that a strong and statistically significant positive linear correlation exists relating the temperature set at the inlet to the air speed ($r = 0.933$) and to the surface temperature difference between the prototype and the control slab ($r = 0.961$ for maximum value and $r = 0.853$ for steady state value). This result is a clear indication that the behaviour of the system can be controlled effectively by setting an appropriate inlet temperature.

Furthermore, a strong and statistically significant positive linear correlation was found relating the temperature set at the inlet to the temperature in the air box (r=0.891). This is an effect of the geometry of the system and is motivated by the fact that air stagnates in the inlet air box, thus, increasing its temperature (for a more detailed discussion about this aspect see Section 4.4). If the geometry of the inlet was different, e.g., if the inlet pipe was connected to the prototype with a manifold, there would be no air accumulation in the inlet air box and the flow regime would clearly be different, thus, the measurement of what is here called $T_{air\ box}$ would not be meaningful.

A less significant but still rather high positive linear correlation was found relating the inlet temperature to the bottom temperature of the asphalt slab (r=0.753). This correlation is due to the fact that the prototype is thermally insulated, thus, if a higher temperature is set at the inlet a higher amount of heat will be accumulated in the pavement layers.

A statistically significant and positive correlation exists relating the surface temperature, T_s, to the temperatures in the pavement layers, i.e. T_{top} (r=0.996) and T_b (r=0.739). This is in accordance with the physics that are considered, as the strong linear correlation in the first layer corresponds to thermal conduction, while the weaker correlation with the temperature at a lower depth is an indication of the additional presence of thermal convection, which is not a linear phenomenon[27].

Finally, it is important to notice that the air speed has a strong and statistically significant positive correlation with the temperature difference between the pavement prototype and the control slab ($r = 0.850$ for maximum value and $r = 0.835$ for steady state value). This is in accordance with the previous literature on energy harvesting pavements, where it was reported that a higher speed improves the heat transfer phenomena due to an increase in the convective heat transfer coefficient [5]. This positive correlation means that a higher temperature increase is reported when the air speed is higher.

	T_s	v_a	T_b	T_{top}	$T_{air\ box}$	T_{set}
T_s	1					
v_a	0.917**	1				
T_b	0.995**	0.932**	1			
T_{top}	0.997**	0.942**	0.996**	1		
$T_{air\ box}$	0.774*	0.516	0.738*	0.739*	1	
T_{set}	0.907**	0.997**	0.928**	0.935**	0.485	1

*Correlation is significant at the 0.05 level (2-tailed).
**Correlation is significant at the 0.01 level (2-tailed).

Legend:
T_s=surface temperature of prototype pavement, v_a= air speed,
T_b= temperature at 50 mm from bottom of prototype pavement,
T_{top}= temperature at 50 mm from surface of prototype pavement,
$T_{air\ box}$= temperature at inlet air box, T_{set}= inlet temperature chosen

Table 4: Pearson's correlation coefficient for the simulation of summer conditions.

4.2.2. Summer conditions

An analysis of the Pearson's correlation coefficient for simulated summer conditions is shown in Table 4. In the case of summer conditions, only the results obtained with the outlet chimney installed are here analysed. The reason for this is that in previous research the authors reported that the absence of a chimney is a negative aspect for the reduction of the pavement temperatures in summer conditions [11, 10] and this was confirmed by the experimental campaign run with the novel experimental setup. To be specific, the absence of a chimney causes the outlet speed to be extremely low, or even null, unless the inlet temperature in very high, thus, the results obtained with no chimney are disregarded as they do not represent the desired conditions tor a functional temperature reducing pavement in the summer. This is because during summer the air mass flow is supposed to be generated by the absortpion of heat from the pavement and only in winter can it be accepted to have an air flow powered by the inlet temperature alone.

The most striking aspect in the data shown in Table 4 is that the correlations between the variables under analysis are mostly linear, as proven by the rather high values of the Pearson's coefficient. Moreover, it is interesting to notice that all the values shown in Table 4 are positive and higher than 0.485, as opposed to those seen in Table 3.

Thus, in the case of simulated summer conditions, the data suggests that the set temperature has a strong and statistically significant correlation with the surface temperature (r=0.907), the air speed (r=0.997), the bottom temperature (r=0.928), and the top temperature (r=0.935). Consequently, a lower inlet temperature will generally cause lower pavement temperatures. If the inlet temperature set is lower, the temperature difference between the pavement and the air flowing in the channels is higher, which causes the heat transfer phenomena to be more effective. For this reason, when the inlet temperature is lower the pavement will be cooler not only because the incoming air is cooler but also as a consequence of a higher rate of heat transfer.

Furthermore, it is relevant to notice that the correlation between air speed and all the pavement temperatures is statistically significant and positive. This can be explained by the fact that when the mass flows of air mix at the outlet before the chimney the resulting mass of air is at a higher temperature when the pavement is hotter, thus, the higher energy content is the reason of a higher air speed at the outlet. It is interesting to point out that the air speed in laboratory simulated winter conditions is not linearly related to the surface temperature (r=-0.079), while in the case of summer it is (r=0.917). This is probably related to the different boundary conditions in the experiments, as in summer an incident heat flux is directly providing energy to the pavement and, therefore, to the air flowing under it, while in winter the air is releasing low-temperature heat to the pavement. This clearly shows that during laboratory simulated summer conditions the air movement is caused by the incident heat flux, and, therefore, by the pavement temperatures, while during winter the velocity is caused by the inlet temperature that is chosen. As a consequence the effect of the heat transfer during winter is hardly seen on the pavement itself, i.e., there is no linear relationship between surface temperature and air speed.

Finally, once again it can be observed that the linear correlation between the surface temperature and the other pavement temperatures is statistically significant and positive. The linear correlation between the temperatures in the domain is the confirmation of the acceptability of the equations shown in Section 3.1 for the description of the relevant physical phenomena happening in the prototype pavement in simulated summer conditions, too. The fact that in simulated summer conditions the correlation between surface temperature and bottom temperature is higher than in winter is likely to be related to the fact that in summer the surface heat flux is far more significant than the convection flux in the pipes. Therefore, the non-linear effect due to thermal convection has less impact on the experimental results.

4.3. Comparison between computational and experimental results

In Fig. 8(a) and Fig. 8(b) the values of air speed obtained with the CFD simulations in winter conditions are shown along with experimental results. The comparison is here presented for winter conditions due to the fact that this allows a more accurate discussion, since configurations both with and without chimney can be considered for the calculation of the outlet air speed. As mentioned in Section 4.2.2, the absence of a chimney in simulated summer conditions results in a null air speed with almost all experimental inlet temperatures. Furthermore, for the purpose of the examination of CFD methods to represent the physical phenomena at work, the use of simulated summer or winter conditions does not make a difference, since the boundary conditions in the computational setup of the problem are selected according to an identical logic.

A visual comparison between the computational and experimental results seen in Fig. 8(a) and Fig. 8(b) suggests that the various experimental configurations can be effectively represented with the methods described in Section 3. In particular, it is important to notice that the fitting lines for experimental and computational results are very close to one another and that the trend in the data is the same. To allow a more accurate comparison the slope and goodness of fit of the lines shown in Fig. 8(a) and Fig. 8(b) can be calculated. The slopes for the experimental results are 0.0181 m/(s°C) and 0.0219 m/(s°C) for the experiments with and without chimney respectively, while the corresponding values of goodness of fit are 0.929 and 0.871. On the other hand, the slopes for the CFD simulations are 0.0182 m/(s°C) and 0.0224 m/(s°C) for the simulations with and without chimney respectively, with goodness of fit of 0.936 and 0.873. These numerical results combined with a visual assessment of Fig. 8(a) and Fig. 8(b) confirm that CFD simulations can be used to describe the phenomena at work in this novel experimental setup, thus, computational studies can be regarded as a good method to provide insight to improve the design of the system.

It is, however, important to mention that an effective simulation of the performance of the technology strictly depends on the choice of the right boundary conditions, which in this paper were fixed based on the experimental values obtained. The aim pursued here was to assess whether CFD simulations could be used to effectively represent the phenomena ruling air flow in the system under analysis or not, thus, the most important target was to match the values of air speed obtained in the laboratory. As a matter of fact, if all the simulations had been performed with the same surface temperature or incident heat flux and the exact same ambient temperature the results would show a smoother evolution. For these reasons, if a prediction of the behaviour of the system under investigation in real life conditions was needed, the input data for the computational model should come from weather databases for a specific location. Such weather data need to include surface temperatures, air temperatures, and soil temperatures at a given depth. In addition, accurate boundary conditions for the inlet and the outlet need to be used to reduce the small mismatch between the experimental and simulated values of air speed seen in Fig. 8(a) and Fig. 8(b) because buoyancy powered flows are highly affected by temperature and pressure gradients in a chosen system.

The CFD simulations performed for this paper were run in steady state conditions as they were meant to reproduce the results obtained in the laboratory, where it is usually possible to reach stable results. This would typically not be possible in the case of a real life installation due to the fact that environmental conditions constantly change and influence the dynamics of the air flow. For this reason it is clear that a steady state simulation is not fit for the study of such a dynamic system in real life conditions, therefore, the use of transient analyses is recommended for the design of practical applications of the technology.

4.4. Further insight and future developments

The good accuracy of the results discussed in Section 4.3 suggest that CFD simulations are fit to describe the fluid dynamics happening in the system under investigation, thus, it is interesting to look at the computational results more closely.

To begin with, in Section 4.2.1, it was mentioned that the air stagnates in the inlet air box. This can be confirmed by examining the particle traces in the computational reproduction of the experimental setup along with the temperature profile in a cross section of the system (see Fig. 9). The particle traces were generated using Autodesk CFD by creating a circular grid of seeds at the system inlet. The traces in Fig. 9(a) are coloured by velocity magnitude, thus, it is possible to see how air interacts with the solid boundaries of the ground source heat simulator. In Fig. 9(a), it can be seen that the air velocity in the inlet air box is very low (close to 0 m/s) and this is due to the geometry of the system: the air comes from the inlet pipe, then it is scattered by the walls of the inlet air box, and finally enters the pipes embedded in the aggregate layer of the prototype pavement. This geometry is functional for a first study of the performance of the system, however, energy is lost by the air in the inlet air box due to friction/eddy effects. As a matter of fact, the same phenomenon is seen in the outlet box where air mass flows mix, thus, the use of optimised geometric configurations should be pursued. The experimental setup described in this paper proved effective. However, it is expected that with a more accurate study of the shape of the air channels a higher performance could be achieved. The effect of stagnation is seen also in the temperature profile shown in Fig. 9(b), where the temperature is close to the inlet temperature chosen (30°C, in this case) across the whole inlet air box. In the outlet box, the same phenomenon is reported, as the air speed is approximately the same in the whole section.

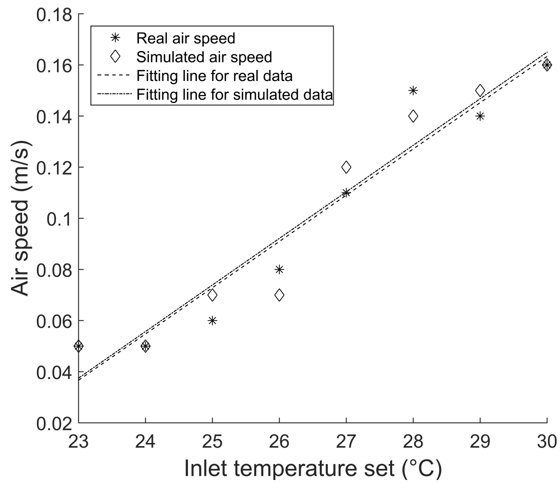

(a) Tests with chimney

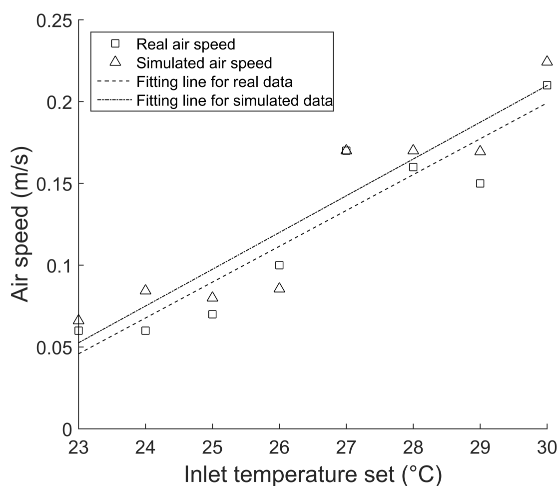

(b) Tests without chimney

Figure 8: Real data vs. computational results (Winter conditions).

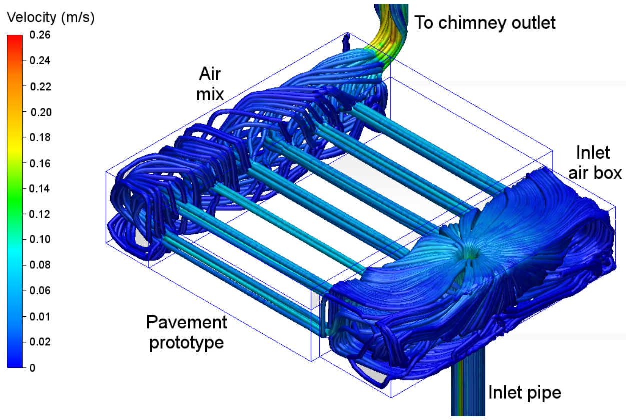

(a) Particle traces with velocity magnitude

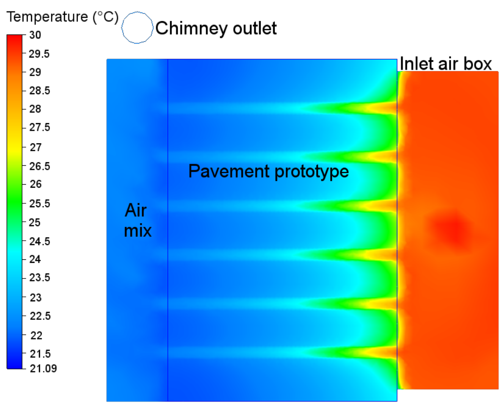

(b) Cross section with temperature profile

Figure 9: Stagnation of air in the inlet air box (Winter conditions).

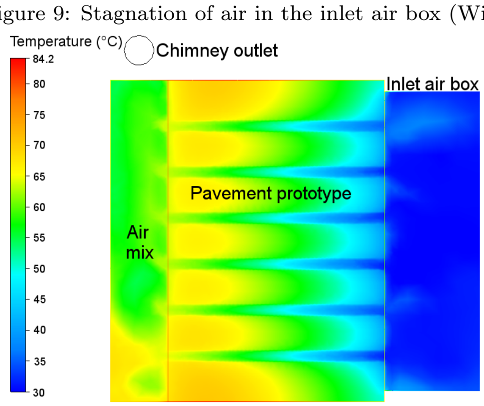

Figure 10: Cross section with temperature profile (Summer conditions).

Furthermore, it is interesting to examine the temperature profile in the pipes shown in Fig. 9(b). A visual analysis of the temperature profile in the pipes shows that the temperature of air is highly affected by the inlet temperature chosen for a certain length, then it decreases thanks to the release of heat to the pavement. A similar phenomenon happens in summer conditions, however, in this case the temperature in the pipes increases through the length of the pipes due to the energy abstraction process (see Fig. 10). In addition, the stagnation phenomenon seen in winter conditions is also present in summer conditions, as shown by the mostly constant inlet box temperature.

5. Preliminary testing in the environment

Since all the experiments mentioned above were performed in a controlled laboratory environment the experimental setup was also tested in real life conditions for 9 days. This was done in order to assess whether the pavement prototype would provide a measurable temperature control effect with varying environmental conditions or not. The testing took place at the University of Nottingham, UK, during the last two weeks of August 2015. The same equipment described in the previous sections was used, setting a sampling interval of 15 minutes in the data logger. Note that the ground source heat simulator was fully weatherproofed, however, no precipitation was recorded throughout this preliminary test. During these 9 days, the environmental temperature ranged between 7°C and 24°C (see Fig. 11), which consistent with late summer temperatures in the area.

The data in Fig. 11 clearly shows that the pavement prototype reached higher surface temperatures than the control slab during cold periods and lower surface temperatures than the control slab during hot periods. For the whole period of time under analysis, daily maximum temperature differences of +6°C and nightly temperature differences of -6°C were found between the control slab and the pavement prototype. This was achieved with an air inlet temperature of 15°C, which is a realistic value for a geothermal heat source, unlike those used

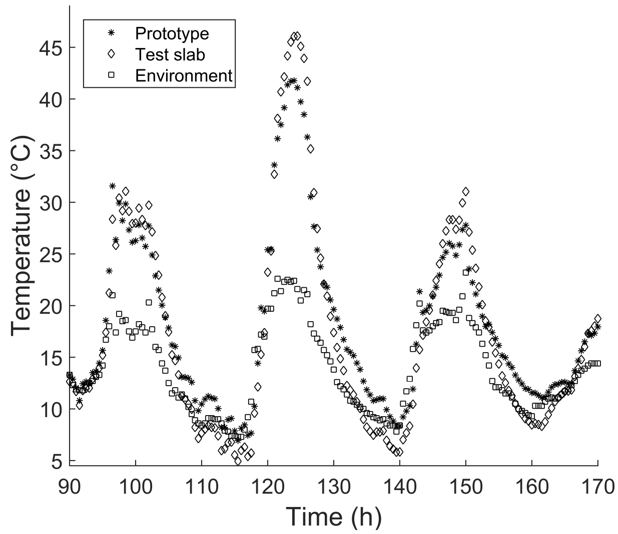

Figure 11: Temperature difference between prototype and control slab (hours 90 to 170).

in the laboratory experiments.

The results obtained during this preliminary testing period are very promising, thus, the authors recommend that further research should focus on a comprehensive analysis of the relationship between the performance of the system and a number of parameters defining the weather conditions, e.g., the air temperature, the air humidity, and the precipitation.

6. Conclusions

In this paper, a novel experimental setup for the analysis of temperature-managed pavements operated by air convection was presented and used to analyse the performance of a pavement prototype from both a statistical and computational point of view.

The following conclusions can be drawn:

- It is possible to simulate a soil temperature by the means of the ground source heat simulator designed.

- The performance of a temperature-managed pavement can be influenced controlling the inlet temperature of air.
- In simulated winter conditions, temperature increases of between 0.4°C and 2.1°C were achieved.
- In simulated summer conditions, temperature decreases of between 2°C and 6°C were achieved.
- Linear relationships between the parameters of interest were found by analysing the Pearson's correlation coefficient. In particular, increasing values of the inlet air temperature were shown to cause an increase in the surface temperature in both simulated winter and summer conditions.
- Computational simulations were identified as an effective mean to describe the physics of temperature-managed pavements powered by air convection.
- The analysis of the results of computational simulations can provide useful insight for the design of this kind of systems, especially about the geometric configuration of the path of air.
- Preliminary testing in real life conditions proved the validity of the approach and its effectiveness. Temperature differences between the pavement prototype and the control slab ranging from about -6°C to +6°C were measured with the experimental equipment.

Acknowledgements

The authors thank the University of Nottingham for the financial support provided for the Ph.D. of Andrea Chiarelli. The authors also acknowledge the assistance provided by John Markowycz during the experimental activities.

7. References

[1] U. Lohmann, R. Sausen, L. Bengtsson, U. Cubasch, J. Perlwitz, E. Roeckner, The Köppen climate classification as a diagnostic tool for general circulation models, Climate Research 3 (1993) 177–193.

[2] H. Wang, J. Zhao, Z. Chen, Experimental investigation of ice and snow melting process on pavement utilizing geothermal tail water, Energy Conversion and Management 49 (2008) 1538–1546. doi:10.1016/j.enconman.2007.12.008.

[3] H. Dai, K. Zhang, X. Xu, H. Yu, Evaluation on the effects of deicing chemicals on soil and water environment, Procedia Environmental Sciences 13 (2012) 2122–2130. doi:10.1016/j.proenv.2012.01.201.

[4] Y. Lai, Y. Liu, D. Ma, Automatically melting snow on airport cement concrete pavement with carbon fiber grille, Cold Regions Science and Technology 103 (2014) 57–62. doi:10.1016/j.coldregions.2014.03.008.

[5] V. Bobes-Jesus, P. Pascual-Muñoz, D. Castro-Fresno, J. Rodriguez-Hernandez, Asphalt solar collectors: A literature review, Applied Energy 102 (2013) 962–970. doi:10.1016/j.apenergy.2012.08.050.

[6] J. S. Golden, K. E. Kaloush, Mesoscale and microscale evaluation of surface pavement impacts on the urban heat island effects, International Journal of Pavement Engineering 7 (2006) 37–52. doi:10.1080/10298430500505325.

[7] J. W. Lund, Pavement snow melting, http://www.oit.edu/docs/default-source/geoheat-center-documents/publications/snow-melting/tp108.pdf?sfvrsn=2, accessed Oct. 14, 2015 (2000).

[8] J. W. Lund, D. H. Freeston, T. L. Boyd, Direct utilization of geothermal energy 2010 worldwide review, Geothermics 40 (2011) 159–180. doi:10.1007/s11252-007-0031-x.

[9] M. A. Cunningham, E. Snyder, D. Yonkin, M. Ross, T. Elsen, Accumulation of deicing salts in soils in an urban environment, Urban Ecosystems 11 (2008) 17–31. doi:10.1007/s11252-007-0031-x.

[10] A. Chiarelli, A. Dawson, A. García, Analysis of the performance of an air-powered energy harvesting pavement, Transportation Research Record: Journal of the Transportation Research Board 2523 (2015) 156–163. doi:10.3141/2523-17.

[11] A. Chiarelli, A. Dawson, A. García, Parametric analysis of energy harvesting pavements operated by air convection, Applied Energy 154 (2015) 951–958. doi:10.1016/j.apenergy.2015.05.093.

[12] D. R. McCaulou and D. G. Jewett and S. G. Huling, Nonaqueous phase liquids compatibility with materials used in well construction, sampling, and remediation, http://www2.epa.gov/sites/production/files/2015-06/documents/napl.pdf, accessed Oct. 14, 2015.

[13] A. Chiarelli, A. Al-Mohammedawi, A. Dawson, A. García, Construction and configuration of convection-powered asphalt solar collectors for the reduction of urban temperatures, International Journal of Thermal Sciences 112 (2017) 242–251. doi:10.1016/j.ijthermalsci.2016.10.012.

[14] P. Pascual-Muñoz, D. Castro-Fresno, P. Serrano-Bravo, A. Alonso-Estébanez, Thermal and hydraulic analysis of multilayered asphalt pavements as active solar collectors, Applied Energy 111 (2013) 324–332. doi:10.1016/j.apenergy.2013.05.013.

[15] A. García, M. Partl, How to transform an asphalt concrete pavement into a solar turbine, Applied Energy 119 (2014) 431–437. doi:10.1016/j.apenergy.2014.01.006.

[16] M. Pomerantz, H. Akbari, A. Chen, H. Taha, A. H. Rosenfeld, Paving materials for heat island mitigation, Ernest orlando lawrence berkeley national laboratory, 1997, LBL-38074.

[17] H. Akbari, L. S. Rose, H. Taha, Characterizing the fabric of the urban environment: A case study of Sacramento, California, U. S. Environmental Protection Agency, 1999, LBNL-44688.

[18] J. Gui, J. Carlson, P. E. Phelan, K. E. Kaloush, J. S. Golden, Impact of pavement thickness on surface diurnal temperatures, Journal of Green Building 2 (2007) 121–130. doi:dx.doi.org/10.3992/jgb.2.2.121.

[19] H. Akbari and A. A. Berhe and R. Levinson and S. Graveline and K. Foley and A. H. Delgado and R. M. Paroli, Aging and weathering of cool roofing membranes, http://escholarship.org/uc/item/3qb8j3k7, accessed Oct. 15, 2015.

[20] A. A. Sarat, M. A. Eusuf, An experimental study on observed heating characteristics of urban pavement, Journal of Surveying, Construction and Property 3 (2012) 1–12.

[21] M. Santamouris, Using cool pavements as a mitigation strategy to fight urban heat island - a review of the actual developments, Renewable and Sustainable Energy Reviews 26 (2013) 224–240. doi:10.1016/j.rser.2013.05.047.

[22] N. A. A. Guntor, M. F. M. Din, M. Ponraj, K. Iwao, Thermal performance of developed coating material as cool pavement material for tropical regions, Journal of Materials in Civil Engineering 26 (2014) 755–760. doi:10.1061/(ASCE)MT.1943-5533.0000859.

[23] E. Carnielo, M. Zinzi, Optical and thermal characterisation of cool asphalts to mitigate urban temperatures and building cooling demand, Building and Environment 60 (2013) 56–65. doi:10.1016/j.buildenv.2012.11.004.

[24] A. Synnefa, T. Karlessi, N. Gaitani, M. Santamouris, D. N. Assimakopoulos, C. Papakatsikas, Experimental testing of cool colored thin layer asphalt and estimation of its potential to improve the urban microclimate, Building

and Environment 46 (2011) 38–44. doi:10.1016/j.buildenv.2010.06.014.

[25] A. Chiarelli, Energy harvesting pavements using air convection, Ph.D. thesis, The University of Nottingham (2016).

[26] A. García, A. Hassn, A. Chiarelli, A. Dawson, Multivariable analysis of potential evaporation from moist asphalt mixture, Construction and Building Materials 98 (2015) 80–88. doi:10.1016/j.conbuildmat.2015.08.061.

[27] F. M. White, Fluid Mechanics, McGraw-Hill, 2002.

[28] P. L. Quéré, C. Weisman, H. Paillère, J. Vierendeels, E. Dick, R. Becker, M. Braack, J. Locke, Modelling of natural convection flows with large temperature differences: A benchmark problem for low mach number solvers. Part 1. Reference solutions, ESAIM: Mathematical Modelling and Numerical Analys 39(3) (2005) 609–616. doi:10.1051/m2an:2005027.

[29] W. K. George, An introduction to natural convection flows, http://www.turbulence-online.com/Publications/Lecture_Notes/Natural_Convection_Lectures.pdf/, accessed Oct. 14, 2015.

[30] H. G. Lee, J. Kim, A comparison study of the Boussinesq and the variable density models on buoyancy-driven flows, Journal of Engineering Mathematics 75 (2011) 15–27. doi:10.1007/s10665-011-9504-2.

[31] M. Medale, A. Haddad, A 3D low mach number model for high performance computations in natural or mixed convection newtonian liquid flows, Journal of Physics: Conference Series 395 (2012) 012095. doi:10.1088/1742-6596/395/1/012095.

[32] J. L. Rodgers, W. A. Nicewander, Thirteen ways to look at the correlation coefficient, The American Statistician 42 (1988) 59–66. doi:10.2307/2685263.

[33] C. J. Ferguson, An effect size primer: A guide for clinicians and researchers, Professional Psychology: Research and Practice 40 (2009) 532–538. doi:10.1037/a0015808.

[34] M. G. Kent, S. Altomonte, P. R. Tregenza, R. Wilson, Temporal variables and personal factors in glare sensation, Lighting Research and Technology.doi:10.1177/1477153515578310.

[35] P. Ahlgren, B. Jarneving, R. Rousseau, Requirements for a cocitation similarity measure, with special reference to pearson's correlation coefficient, Journal of the American Society for Information Science and Technology 54 (2003) 550–560. doi:10.1002/asi.10242.

[36] G. D. Ruxton, M. Neuhäuser, When should we use one-tailed hypothesis testing?, Methods in Ecology and Evolution 1 (2010) 114–117. doi:10.1111/j.2041-210X.2010.00014.x.